NACA RM E56I26a

NACA

RESEARCH MEMORANDUM

INVESTIGATION OF SHOCK - BOUNDARY-LAYER INTERACTION ON THE SPIKE OF A CONICAL-SPIKE NOSE INLET

By George A. Wise and William H. Sterbentz

Lewis Flight Propulsion Laboratory
Cleveland, Ohio

NATIONAL ADVISORY COMMITTEE
FOR AERONAUTICS

WASHINGTON
January 9, 1957
Declassified February 8, 1960

NACA RM E56I26a

NATIONAL ADVISORY COMMITTEE FOR AERONAUTICS

RESEARCH MEMORANDUM

INVESTIGATION OF SHOCK - BOUNDARY-LAYER INTERACTION ON THE SPIKE OF A CONICAL-SPIKE NOSE INLET

By George A. Wise and William H. Sterbentz

SUMMARY

Measurements were made of the height of the shock-induced boundary-layer thickening and separation on the spike of a full-scale inlet over a Mach number range of 1.6 to 2.0.

The behavior of the interaction depended on longitudinal spike position as well as on cone surface Mach number. The cone position affected the interaction by changing the rate of subsonic diffusion and thereby changing the pressure aft of the terminal shock. When the pressure rise due to the interaction exceeded about 1.9, the boundary layer was separated.

INTRODUCTION

The performance of an efficient supersonic inlet depends in part upon the characteristics of the boundary layer that is formed on the compression surface. This boundary layer can be thickened or separated as a result of interacting with the inlet terminal shock, and this can seriously compromise the inlet performance.

Other workers have investigated the characteristics of the shock - boundary-layer interaction (refs. 1 and 2) and have presented criteria for determining the onset of separation. The height of the thickened or separated boundary layer is not available, however; and knowledge of this height is needed in order to control the boundary layer at the throat of the supersonic inlet, for example, by means of a boundary-layer scoop or bleed. Therefore, an investigation was conducted to measure the height of a boundary layer having shock-induced thickening and separation on the centerbody of a full-scale conical-spike nose inlet. The inlet, designed to supply air to an operating turbojet engine, had interchangeable spikes with half-angles of 20°, 25°, and 30°. The investigation covered a free-stream Mach number range of 1.6 to 2.0 at zero angle of attack.

SYMBOLS

A_{in}	inlet capture area
D	duct diameter at cowl lip
d	axial distance from cone tip
h	duct height at rake station (normal to flow)
M_d	Mach number at which the oblique shock generated by conical spike intersects cowl lip
M_S	cone surface Mach number
M_0	free-stream Mach number
m_3/m_0	diffuser mass-flow ratio, $\frac{\text{inlet mass flow}}{\rho_0 V_0 A_{in}}$
p_c	static pressure on cone
p_0	free-stream static pressure
V_0	free-stream air velocity
x_R	surface distance of survey rake from cone tip
x_s	surface distance of terminal shock from cone tip
y	cone radius
δ	boundary-layer height
θ_c	cone half-angle
ρ_0	free-stream density

APPARATUS AND PROCEDURE

A drawing of the inlet portion of the model is presented in figure 1, and coordinates of the spikes are presented in table I. The spikes were capable of being translated along the axis of symmetry, and the resulting diffuser area variations for various positions of the spike are presented in figure 2. The position of the spikes is indicated by a design Mach number M_d, which is the Mach number at which the oblique shock from the spike tip would just intersect the cowl lip.

Instrumentation consisted of a row of static-pressure orifices along the spike and a total-pressure rake located as shown in the table on figure 1. The boundary-layer rake was located 45° from the row of statics in order to prevent interference. A sharp static-pressure rise measured by the static-pressure orifices was taken to be the terminal-shock position, and boundary-layer heights were obtained from the rake as shown in sketch (a). The presence of separation was determined by the shape of the rake profiles.

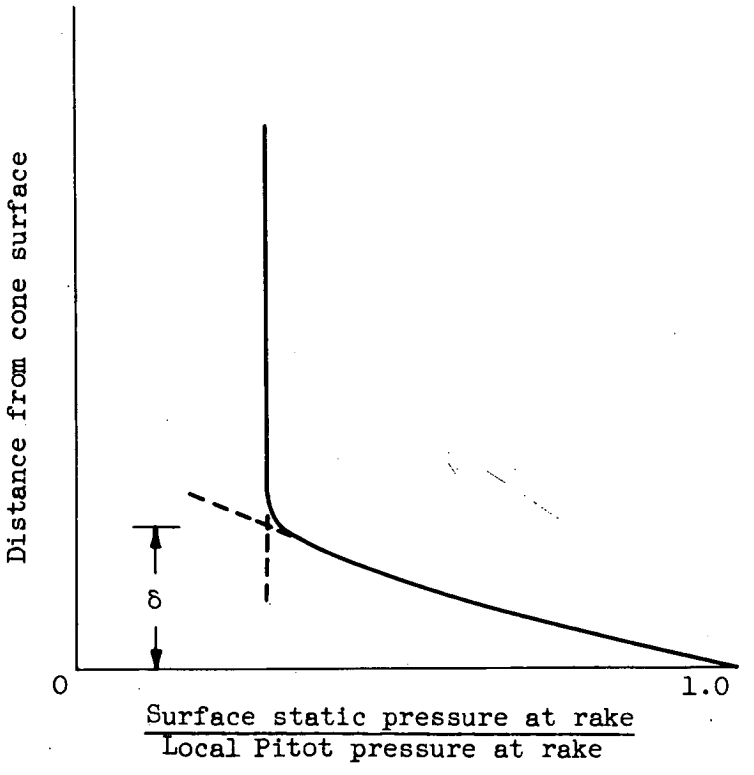

Sketch (a)

The spike was perforated with 1/4-inch-diameter holes just aft of the total-pressure rake. These holes were used in another boundary-layer-bleed study that was run simultaneously with this test. There were eight circumferential rows of holes 5/8 inch apart with 64 holes to

the row. The net flow through these holes was controlled by a single valve, which was kept closed during the portion of the test reported herein. It is thought from previous experience that these perforations had little, if any, effect on the test results.

Data were obtained in the Lewis 8- by 6-foot supersonic tunnel over a Mach number range of 1.6 to 2.0 at zero angle of attack. Reynolds number of the test varied between 5.3×10^6 and 5.9×10^6 per foot.

RESULTS AND DISCUSSION

The boundary-layer heights measured at the rake station are presented in figure 3 as a function of terminal-shock position. The thickness of the undisturbed boundary layer at the rake station is shown at $x_s/x_R = 1.0$. As the terminal shock was forced upstream of this fixed station, the changes in boundary-layer thickness at this station are indicated at values of x_s/x_R less than 1.0. At $x_s/x_R = 0$, the terminal shock would be located at the tip of the cone.

The basic data from figure 3 are cross-plotted in figure 4 to show the rate of growth of the boundary layer as the terminal shock was moved upstream from the rake station. The negative sign on the growth-rate parameter is a result of measuring shock position from the cone tip rather than from the rake; however, an increase in the absolute value of the parameter indicates a more rapid thickening of the boundary layer with shock movement. The rates of growth were calculated at $x_s/x_R = 1.0$. Figure 4 shows that interaction of the terminal shock with the boundary layer caused increased thickening and, ultimately, separation as the free-stream Mach number increased. It can also be seen that increased thickening or separation of the boundary layer takes place with a decrease in cone angle. Both of these phenomena indicate that the characteristics of the interaction were a function of the cone surface Mach number. Generally, the higher the cone surface Mach number, the greater the thickening of the boundary layer due to the interaction and the greater the probability of separation.

Longitudinal spike position also affected the behavior of the shock - boundary-layer interaction. With the inlet terminal shock located at the same position on the spike, the tendency of the boundary layer to separate became greater as the spike was moved upstream. This is shown in figure 4(b) by the separation at the greater tip projections and the absence of such separation at the lower tip projections at free-stream Mach numbers of 1.9 and 2.0. This phenomenon is not noticeable on the 20° cone (fig. 4(a)), because the boundary layer is separated at all Mach numbers except 1.6; and it is not noticeable on the 30° cone (fig. 4(c)), because the flow never separated.

Schlieren photographs illustrating the phenomenon described in the previous paragraph are shown in figure 5, wherein the differences in the boundary-layer behavior with spike position can readily be seen. Conditions are essentially the same between the two photographs except for the spike position; and it can be seen that there is extensive separation when the spike is in the upstream position ($M_d = 2.33$) but only a slight thickening of the boundary layer when the spike is in the retracted position ($M_d = 1.83$). The asymmetry in the flow that is especially noticeable at $M_d = 2.33$ resulted from a slight misalinement of the spike. Though asymmetrical, the flow was steady. At $M_d = 2.33$, a further reduction in mass flow from the point shown caused the inlet to go into buzz; but the flow at $M_d = 1.83$ was stable over the entire available mass-flow range.

Figure 6 shows typical behavior of the static-pressure distribution on the spike as separation occurs due to an upstream translation of the spike. The static-pressure rise across the interaction is about 1.87 for the unseparated case and about 2.2 for the separated. This latter value is larger than the value of about 1.9 quoted in references 1 and 2 as necessary for separation. The increase in the pressure rise when the spike is translated forward is believed to be caused by the increased rate of subsonic diffusion (fig. 2). Thus, it is indicated that downstream influences can affect the behavior of the shock - boundary-layer interaction.

CONCLUDING REMARKS

An investigation was conducted to determine the height of the separated or thickened boundary layer in the region of the throat of a full-scale conical-spike nose inlet after interaction with the inlet terminal shock.

The interaction between the inlet terminal shock and the spike boundary layer was influenced by the position of the spike. Movement of the spike upstream increased the pressure level aft of the terminal shock enough to cause separation of the spike boundary layer in cases where the shock alone was not strong enough to do so.

Lewis Flight Propulsion Laboratory
National Advisory Committee for Aeronautics
Cleveland, Ohio, October 3, 1956

REFERENCES

1. Nussdorfer, T. J.: Some Observations of Shock-Induced Turbulent Separation on Supersonic Diffusers. NACA RM E51L26, 1954.

2. Bogdonoff, S. M., and Kepler, C. E.: Separation of a Supersonic Turbulent Boundary Layer. Rep. No. 249, Dept. Aero. Eng., Princeton Univ., Jan. 1954. (Contract No. N6-onr-270, Task Order 6, Proj. No. NR-061-049).

TABLE I. - COORDINATES OF SPIKES

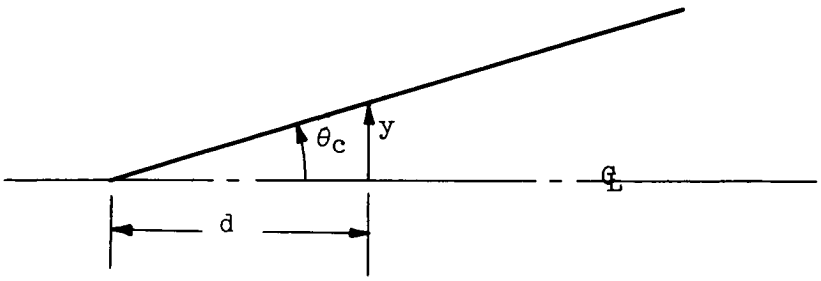

$\theta_c = 20^\circ$		$\theta_c = 25^\circ$		$\theta_c = 30^\circ$	
d,in.	y,in.	d,in.	y,in.	d,in.	y,in.
0	0	0	0	0	0
Straight line		Straight line		Straight line	
18.5	6.71	11	5.12	7.5	4.30
20	7.20	12	5.59	10.0	5.55
22	7.79	14	6.38	12.0	6.37
24	8.22	16	7.07	14.0	7.07
26	8.53	18	7.66	16.0	7.66
28	8.75	20	8.12	18.0	8.10
30	8.90	22	8.48	20.0	8.47

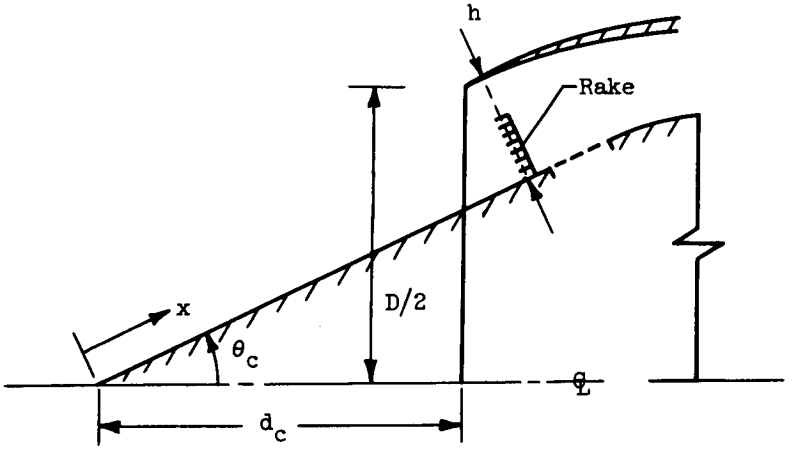

M_d	$\theta_c = 20^\circ$		$\theta_c = 25^\circ$		$\theta_c = 30^\circ$	
	h	d_c	h	d_c	h	d_c
2.3	3.75	12.65	3.34	10.73	3.28	8.91
2.0	4.25	11.10	3.88	9.48	3.88	7.80
1.8	4.59	9.84	4.22	8.42	4.13	6.82
1.6	4.88	8.38	4.63	7.04	4.59	----

θ_c	x_R	D
20°	13.56	17.24
25°	12.28	17.44
30°	10.63	17.44

Figure 1. - Details of model (all dimensions in inches).

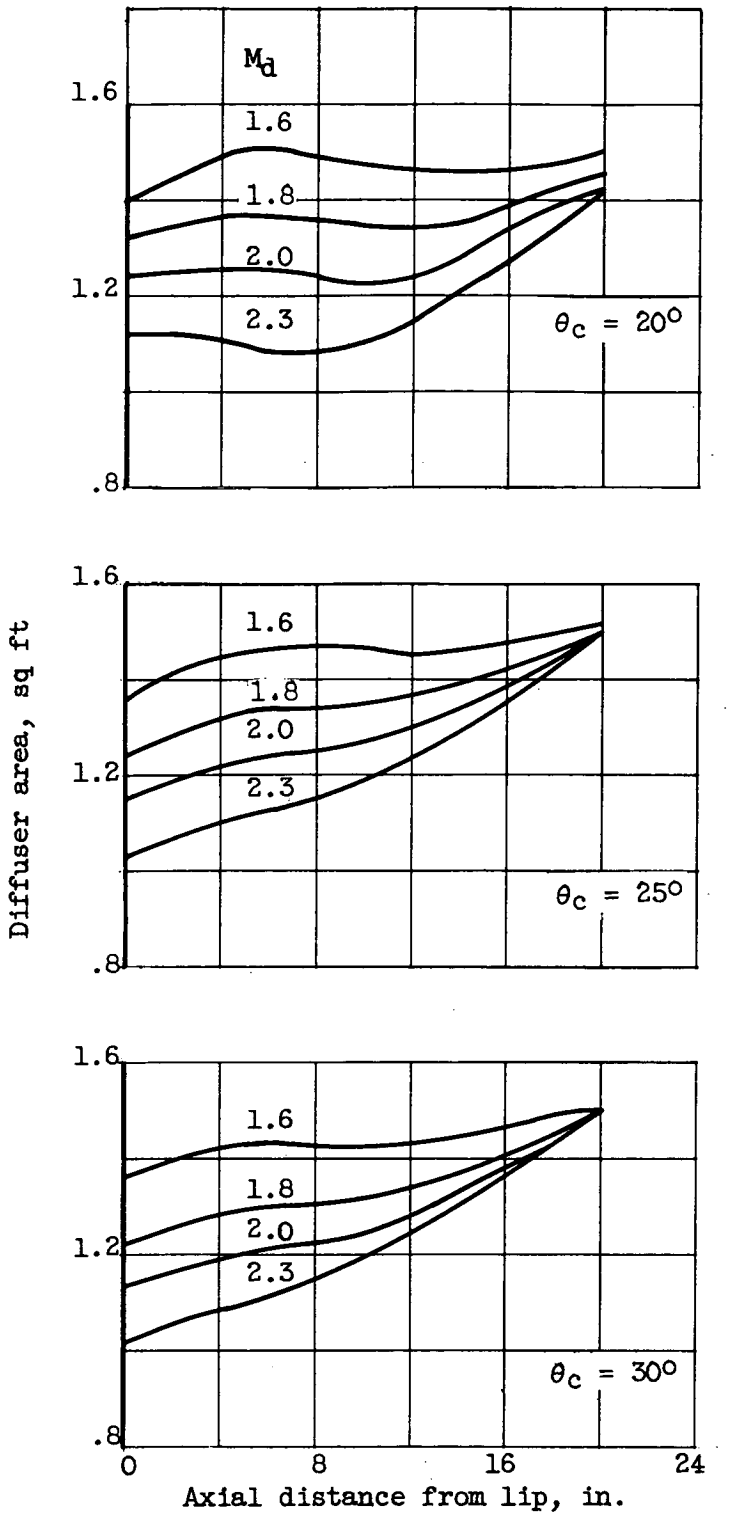

Figure 2. - Diffuser area variations.

(a) 20° Cone. $M_0 = 1.6$; $M_s = 1.24$.

Figure 3. - Variation of boundary-layer height with shock position.

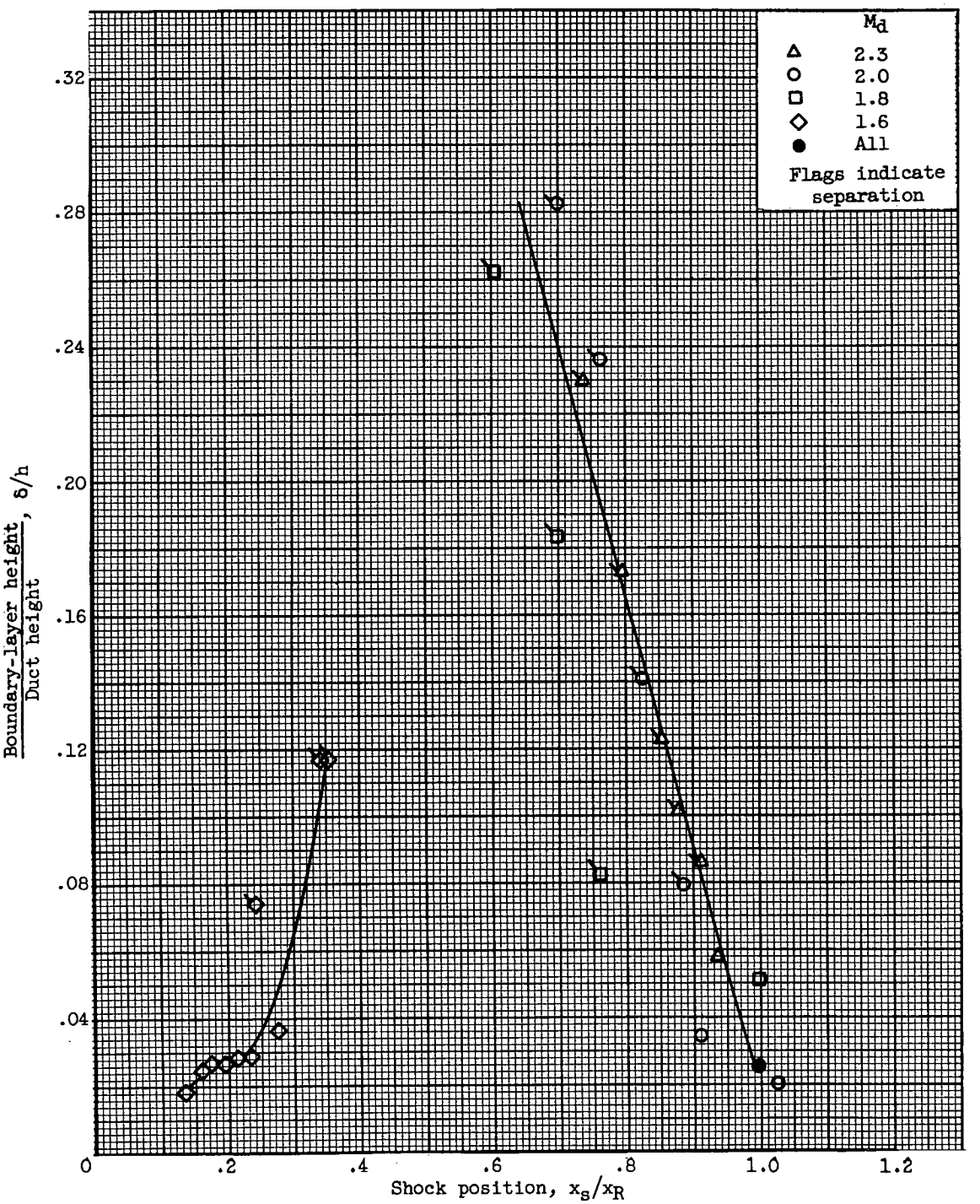

(b) 20° Cone. $M_0 = 1.8$; $M_s = 1.41$.

Figure 3. - Continued. Variation of boundary-layer height with shock position.

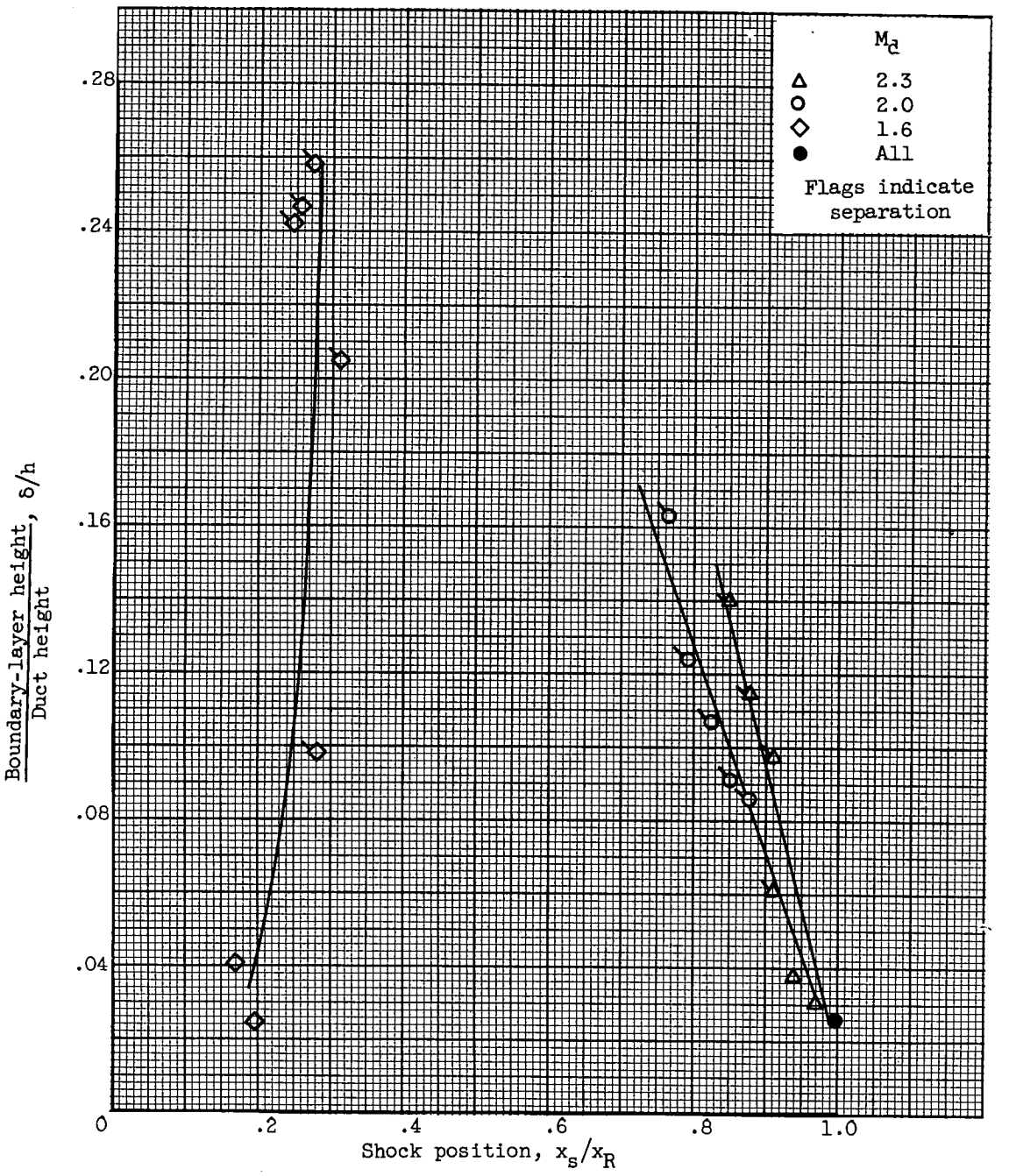

(c) 20° Cone. $M_0 = 2.0$; $M_S = 1.57$.

Figure 3. - Continued. Variation of boundary-layer height with shock position.

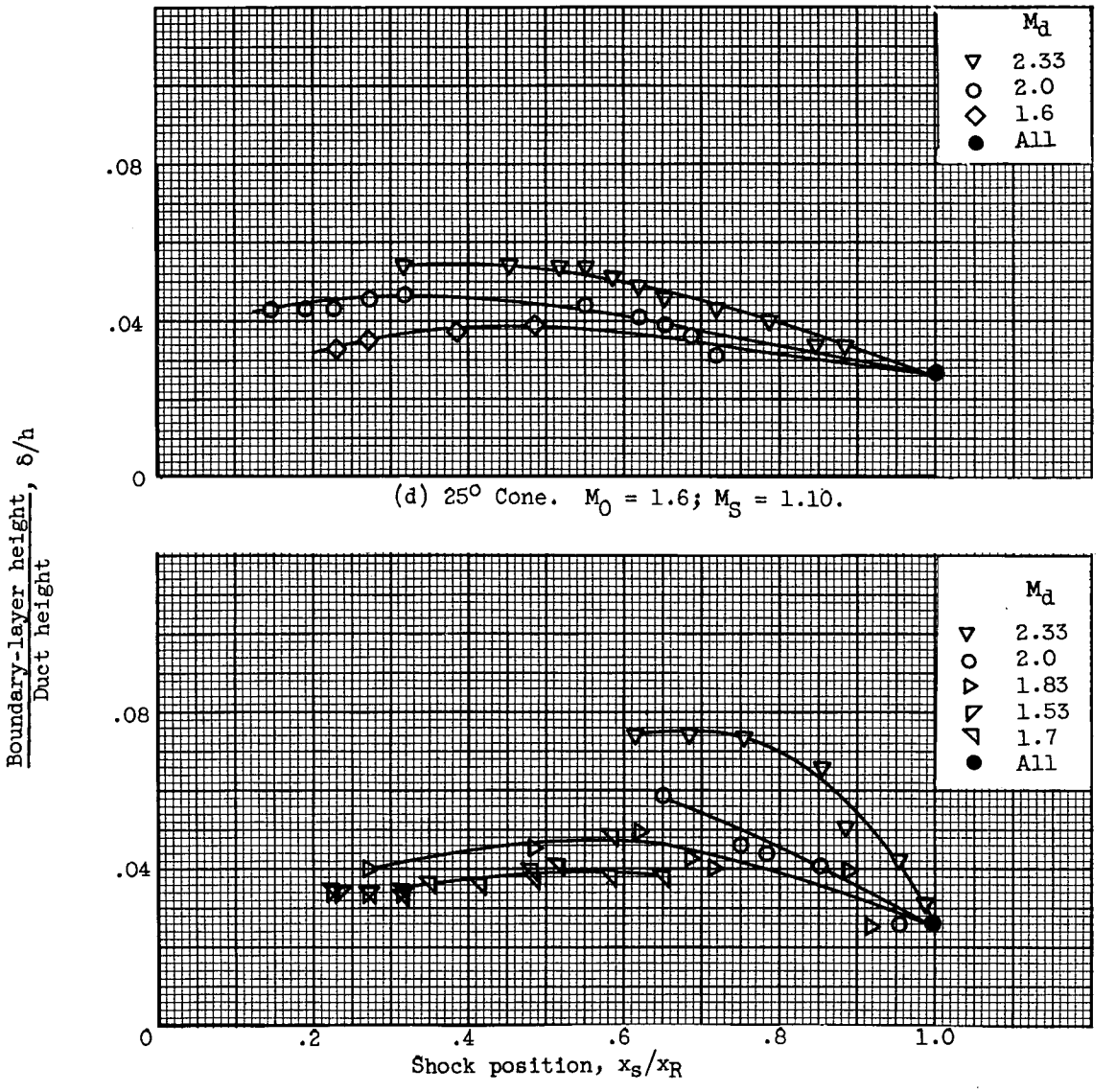

Figure 3. - Continued. Variation of boundary-layer height with shock position.

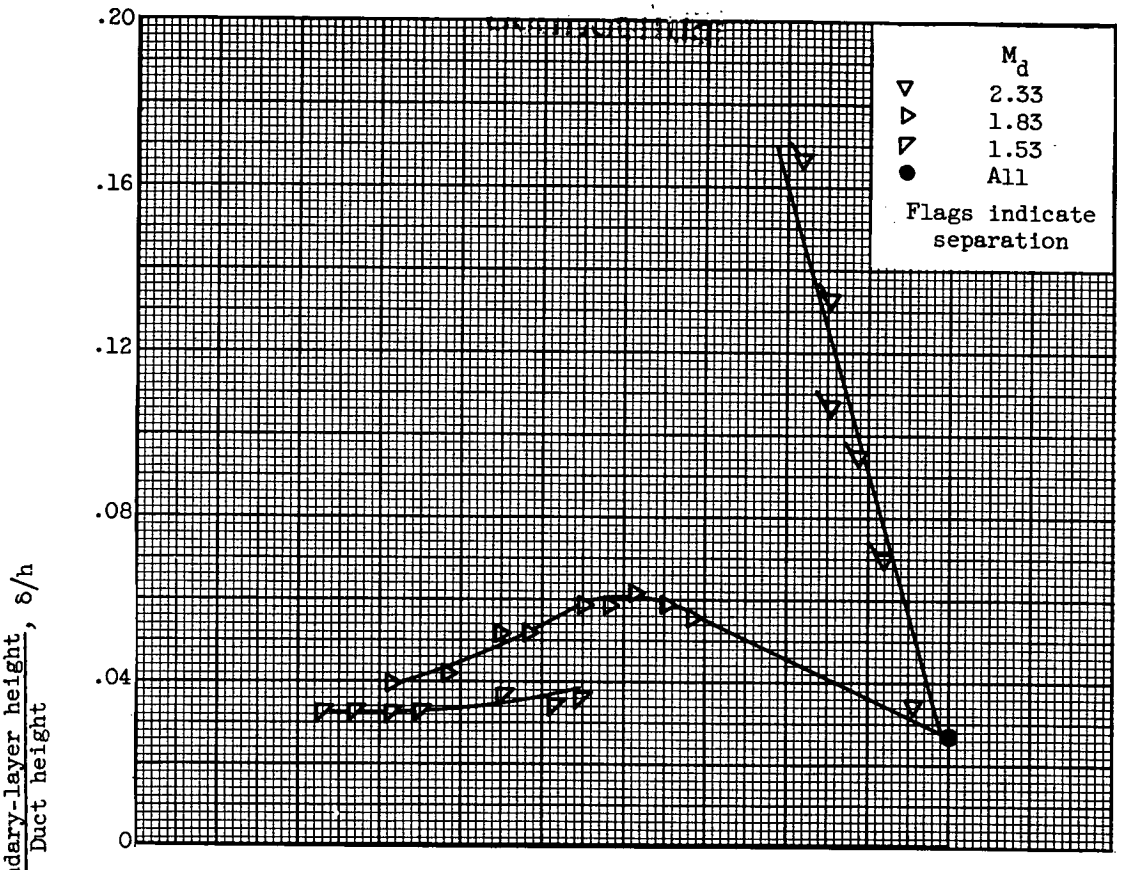

(f) 25° Cone. $M_0 = 1.9$; $M_S = 1.34$.

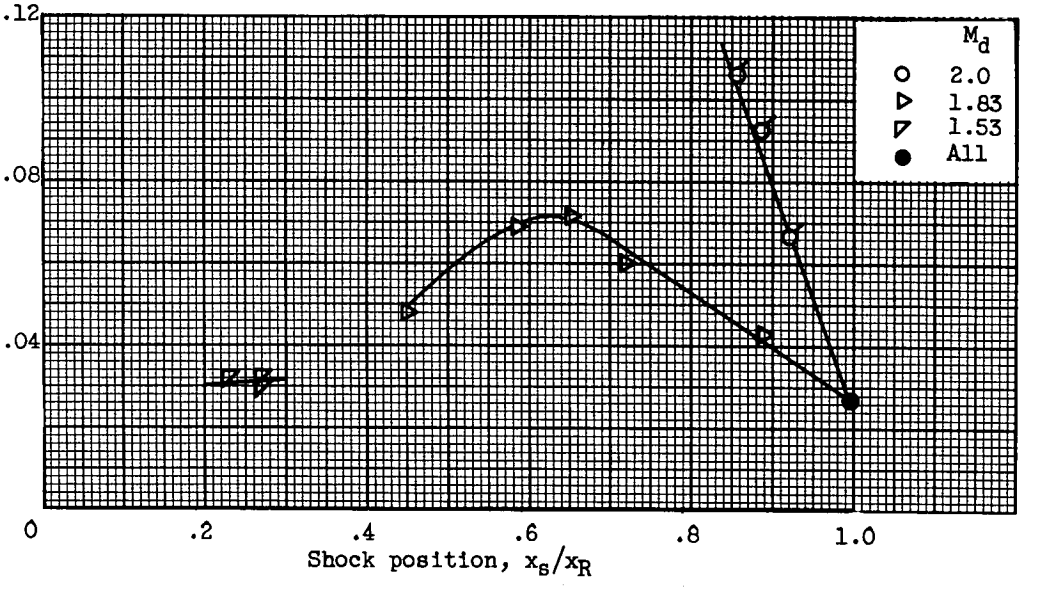

(g) 25° Cone. $M_0 = 2.0$; $M_S = 1.42$.

Figure 3. - Continued. Variation of boundary-layer height with shock position.

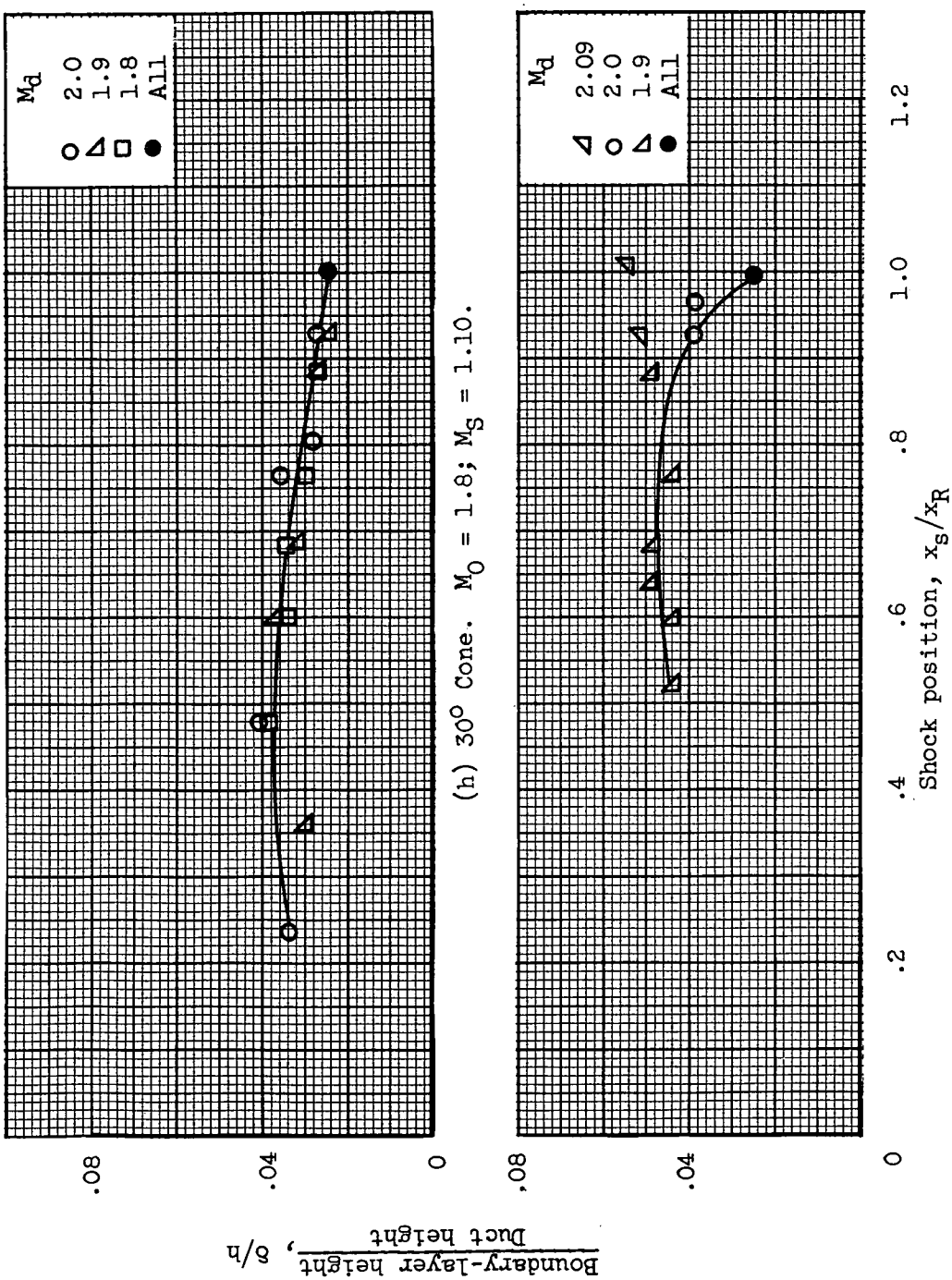

Figure 3. - Concluded. Variation of boundary-layer height with shock position.

(a) Spike half-angle, 20°. (b) Spike half-angle, 25°. (c) Spike half-angle, 30°.

Figure 4. - Behavior of boundary-layer height with shock position as function of free-stream Mach number.

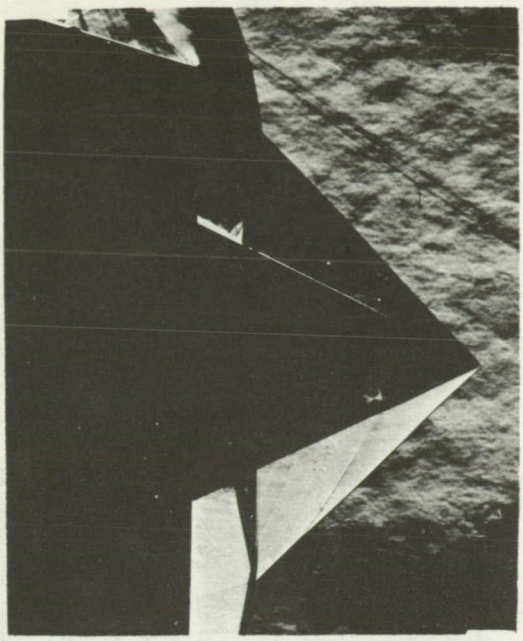

(a) M_d = 1.83.

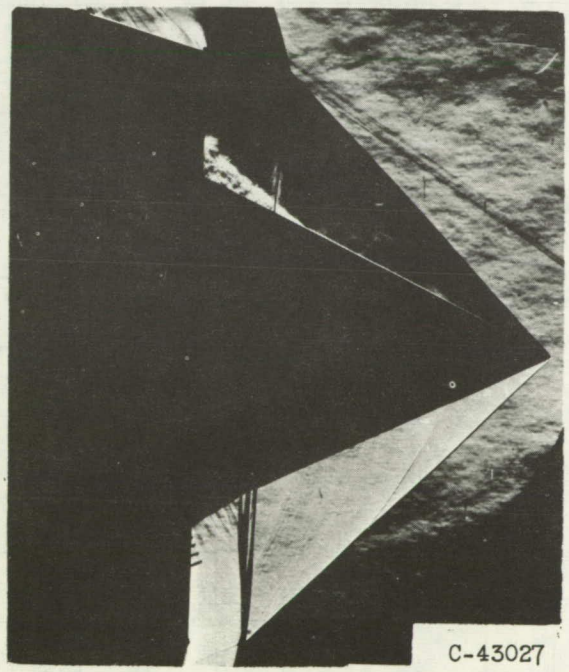

(b) M_d = 2.33.

Figure 5. - Schlieren photographs of 25° cone at free-stream Mach number of 1.9.

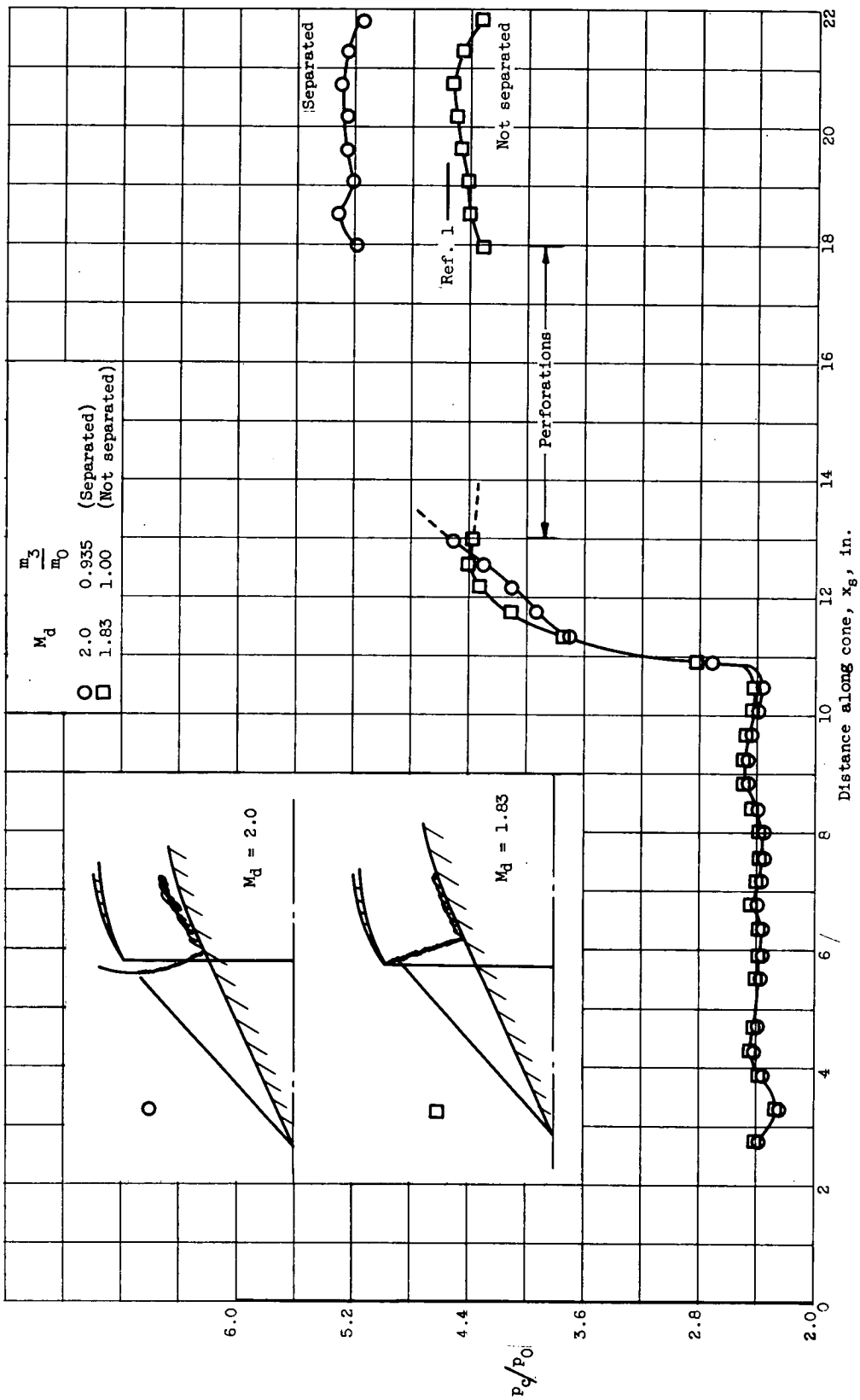

Figure 6. - Static-pressure distribution on 25° cone at free-stream Mach number of 2.0.